Chromothripsis in Healthy Individuals Affects Multiple Protein-Coding Genes and Can Result in Severe Congenital Abnormalities in Offspring

Mirjam S. de Pagter,[1] Markus J. van Roosmalen,[1] Annette F. Baas,[1] Ivo Renkens,[1] Karen J. Duran,[1] Ellen van Binsbergen,[1] Masoumeh Tavakoli-Yaraki,[1,3] Ron Hochstenbach,[1] Lars T. van der Veken,[1] Edwin Cuppen,[1,2] and Wigard P. Kloosterman[1,*]

Chromothripsis represents an extreme class of complex chromosome rearrangements (CCRs) with major effects on chromosomal architecture. Although recent studies have associated chromothripsis with congenital abnormalities, the incidence and pathogenic effects of this phenomenon require further investigation. Here, we analyzed the genomes of three families in which chromothripsis rearrangements were transmitted from a mother to her child. The chromothripsis in the mothers resulted in completely balanced rearrangements involving 8–23 breakpoint junctions across three to five chromosomes. Two mothers did not show any phenotypic abnormalities, although 3–13 protein-coding genes were affected by breakpoints. Unbalanced but stable transmission of a subset of the derivative chromosomes caused apparently de novo complex copy-number changes in two children. This resulted in gene-dosage changes, which are probably responsible for the severe congenital phenotypes of these two children. In contrast, the third child, who has a severe congenital disease, harbored all three chromothripsis chromosomes from his healthy mother, but one of the chromosomes acquired de novo rearrangements leading to copy-number changes. These results show that the human genome can tolerate extreme reshuffling of chromosomal architecture, including breakage of multiple protein-coding genes, without noticeable phenotypic effects. The presence of chromothripsis in healthy individuals affects reproduction and is expected to substantially increase the risk of miscarriages, abortions, and severe congenital disease.

Complex chromosomal rearrangements (CCRs) underlie congenital abnormalities and are thought to be an important contributor to spontaneous abortions in females and to infertility in males.[1–4] Phenotypically normal individuals harboring CCRs have been described, but typically have a copy-number-balanced profile and less-complex rearrangements than phenotypically abnormal individuals. Chromothripsis represents an extreme form of CCRs and has previously been linked to cancer and severe congenital abnormalities. The phenomenon is characterized by local shattering of one or multiple chromosomes and random reassembly of the fragments and typically has a devastating effect on chromosomal architecture and a major impact on human health.[5–9]

We further examined the genomes of two previously described children referred to our Medical Center for a variety of complex congenital abnormalities, and we also investigated the genome of one additional child (Table S1)[8,10,11]. We obtained appropriate informed consent from the involved subjects to analyze their genomes and publish the findings. By using Illumina BeadChip arrays or custom Agilent 105k microarrays, we identified from two to five de novo copy-number changes per child; changes ranged in size from 150 kb to 27 Mb and involved 2 or 3 chromosomes per child (Figure S1). Giemsa (G)-banded chromosome analysis revealed the presence of CCRs involving 1–3 chromosomes in each of the three children (Figures S2A–S2D). Chromosome analysis of the parents showed that in all three cases the mother's karyotype contained all derivative chromosomes identified in her child (Figures S2E–S2H), whereas each of the three fathers displayed a normal karyotype. Furthermore, we identified an additional three derivative chromosomes in the mother of child 1 and one additional derivative chromosome in the mother of child 2 (Figures S2F and S2G). Karyotyping did not reveal any differences between derivative chromosomes identified in child 3 and her mother (Figures S2D and S2H), but previously published FISH (fluorescence in situ hybridization) studies identified de novo rearrangements occurring in the child and resulting in the de novo deletion and duplication.[11] Notably, mothers 1 and 3 are healthy, whereas mother 2 displays a much milder phenotype than her affected child; this phenotype consists of delayed psychomotor development and major learning difficulties but no facial dysmorphisms.[10] We analyzed chromosome spreads from at least 20 lymphocytes and did not find evidence for mosaicism in the mothers.

To further explore the complexity of the chromosomal rearrangements, we performed whole-genome mate-pair sequencing for all three children and their mothers (Table S2).[7,8] We selected breakpoints by filtering data for these three mother-child pairs against a set of 150 control mate-pair datasets and against data from the Genome of the Netherlands Project.[12] In addition, we performed

[1]Department of Medical Genetics, Center for Molecular Medicine, University Medical Center Utrecht, Utrecht 3584 CG, the Netherlands; [2]Hubrecht Institute-Royal Netherlands Academy of Arts and Sciences and University Medical Center Utrecht, Utrecht 3584 CT, the Netherlands
[3]Present address: Department of Biochemistry, Faculty of Medicine, Iran University of Medical Sciences, Tehran 1449614535, Iran
*Correspondence: w.kloosterman@umcutrecht.nl
http://dx.doi.org/10.1016/j.ajhg.2015.02.005. ©2015 by The American Society of Human Genetics. All rights reserved.

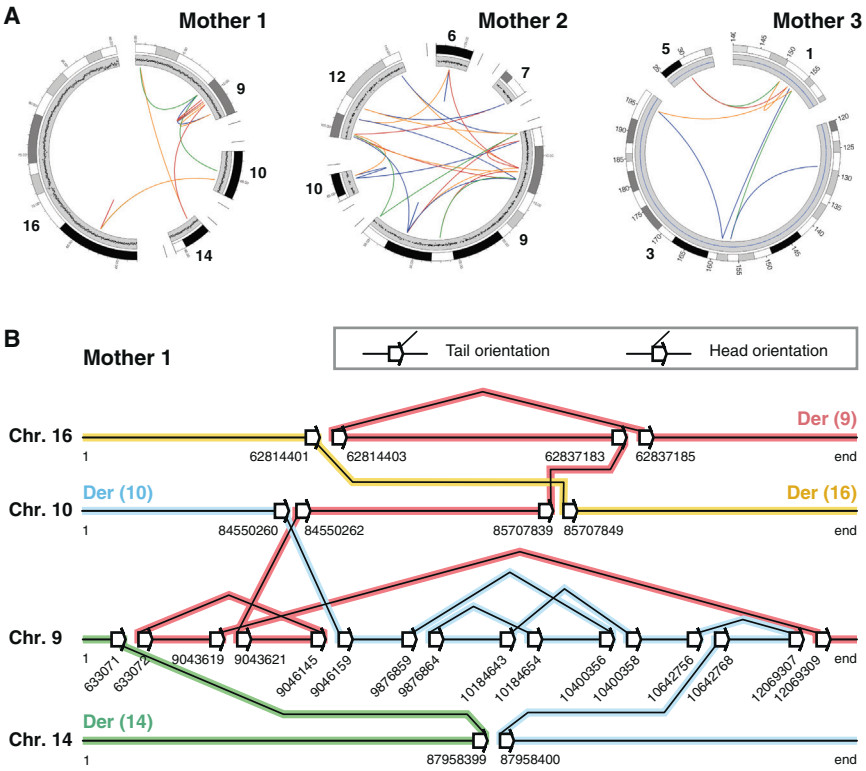

Figure 1. Chromothripsis Involving Multiple Chromosomes Can Be Stably Present in Healthy Individuals

(A) Circos plots of breakpoint junctions (solid lines) in the three mothers. Lines are colored according to the orientation of the breakpoint junction, from low to high chromosomal coordinate: tail-head (blue), head-tail (green), head-head (red), and tail-tail (orange). 13, 23, and 8 rearrangements were detected in mothers 1, 2, and 3, respectively.

(B) Schematic diagram showing the exact genomic positions and orientations of breakpoint junctions detected in mother 1. Sets of adjacent white arrows indicate a double-strand break (DSB), and connecting lines between two arrows indicate breakpoint junctions. This panel shows our rationale for resolving chromosomal structure on the basis of the breakpoint junctions. We produced digital karyotypes by following the breakpoint junctions. By doing so, we predicted that the breakpoint junctions in mother 1 gave rise to four derivative chromosomes, indicated by the colored lines: der(9) (red), der(10) (blue), der(14) (green), and der(16) (yellow). This configuration is fully in line with the karyotypes derived from G-banded chromosome analysis (Figure S2).

validation assays with PCR and Sanger sequencing. We identified 13 (mother 1), 23 (mother 2), and 8 (mother 3) unique breakpoint junctions in the mothers; their sequences are consistent with non-homologous repair mechanisms (Figure 1A, Table S2). Furthermore, plotting of the breakpoint junctions onto the reference genome revealed signatures of double-stranded DNA breaks (Figure 1B, Figure S3). We used the orientations and positions of the breakpoint junctions to reconstruct digital karyotypes, resulting in four derivative chromosomes for mother 1 and five for mother 2 (Figure 2).[6–8,13] We were unable to completely reconstruct the derivative chromosomes for mother 3; probably, we missed some breakpoint junctions because the repetitive character of the affected genomic regions (e.g., 3q29) hampered the unique mapping of sequence reads (Figure S3B). The reconstructed chromosomes match the G-banded chromosome analysis for mother 1 (Figure 2A). However, mate-pair sequencing revealed that five (chr6, chr7, chr9, chr10, and chr12) rather than two chromosomes were involved in the rearrangements in mother 2, emphasizing the importance of next-generation sequencing for revealing the full complexity of the rearrangements (Figure 2B). Taken together, the presence of large numbers of clustered double-stranded breaks affecting a single haplotype, the randomness of breakpoint-junction orientations and DNA-segment order, and the ability to walk the derivative chromosomes provide strong evidence that the rearrangements in the three mothers and their children resulted from germline chromothripsis (Figure 1B, Figure S3A, Table S3).[13] Regularly oscillating copy-number states—typical for cancer chromothripsis—were not observed, consistent with the more balanced state of previously described germline-chromothripsis–affected individuals. Seven out of 13 published cases are completely balanced, whereas the other six cases show only 2–4 copy-number changes.[6–8,14,15] The more balanced state of germline chromothripsis is generally thought to be a consequence of selective pressure during embryogenesis.[6,16]

The large numbers of breakpoints in each of the three mothers, and the lack of a phenotype in two of them, raised the question of whether breakpoints affected their gene function. By examining the overlap between breakpoints and protein-coding genes, we found that 3, 9, and 13 genes have breakpoints in, or in close proximity (<20 kb distance) to, such a gene in mothers 1, 2, and 3, respectively (Figure 3, Figure S4A, Table S4). The affected genes contain breakpoints in introns (14 genes), exons (one gene), the promoter region (five genes), or the 3′ region of the gene (five genes). Five of the affected genes are annotated as disease-associated genes in OMIM; three of these are found in mother 2, who suffers from delayed psychomotor development and major learning difficulties (Table S1). Seven genes are affected by intronic or exonic breakpoints in the two healthy mothers (mothers 1 and 3; Figures 3B and 3C). Because all gene disruptions are heterozygous, next we tested for the probability of haploinsufficiency of the affected genes by applying a metric previously described by Huang et al.[17] This did not categorize any of the genes as very likely to be haploinsufficient, consistent with the absence of a phenotype in two out of three mothers (Figure S4B). In addition, we examined exome sequencing

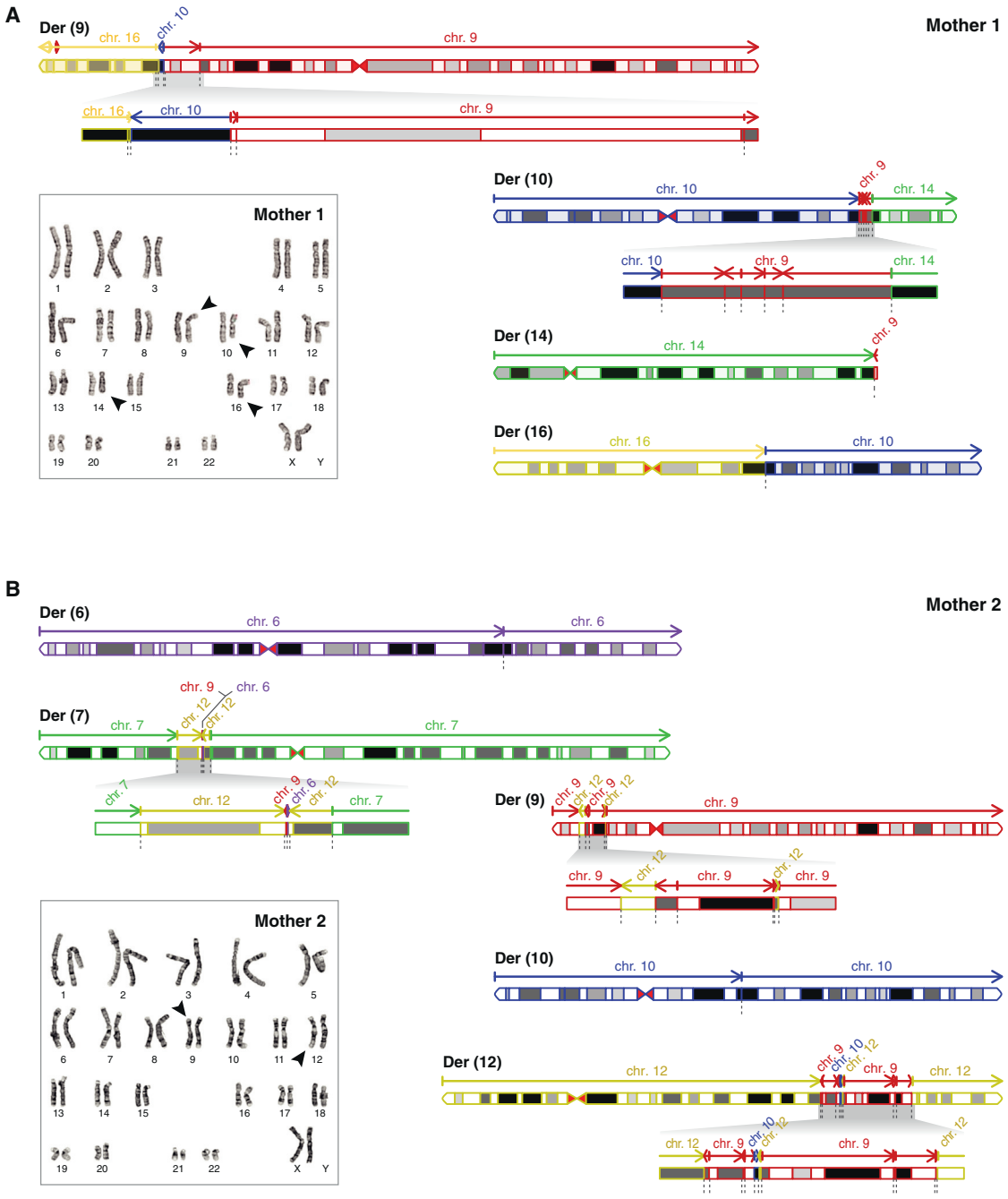

Figure 2. Reconstruction of Digital Karyotypes Based on the Breakpoint Junctions in Mothers 1 and 2
(A) Karyogram and digital karyotype as derived from the sequencing data of mother 1. Chromosome segments are colored according to their origin: chr9 (red), chr10 (blue), chr14 (green), and chr16 (yellow). Der(9) and der(10) harbor a region with a large number of small rearranged fragments (zoom panels). Arrows indicate the orientation of the chromosomal fragments; dotted gray lines indicate breakpoint junctions. The predicted structure of the rearranged chromosomes matches the G-banded karyotype of the mother.
(B) Karyogram and digital karyotype as derived from sequencing data of mother 2. Chromosome segments are colored according to their origin: chr6 (purple), chr7 (green), chr9 (red), chr10 (blue), and chr12 (yellow). Der(7), der(9), and der(12) each harbor one or multiple regions with a large number of small rearrangements (zoom panels). In contrast to that of mother 1, karyotyping of mother 2 revealed only two [der(9) and der(12)] out of five derivative chromosomes detected by mate-pair sequencing (Figure S2G).

data from the Exome Aggregation Consortium (ExAC) and found that multiple loss-of-function mutations are reported for 22/25 affected genes (Figure S4C). Previous studies have shown that every human genome contains around 100 loss-of-function variants.[18] Our data further emphasize the permissiveness of the genome to gene-disrupting changes and to massive relocations of chromosomal segments within a single, healthy individual.

After the reconstruction of the digital karyotypes, we set out to determine the link between the chromothripsis in

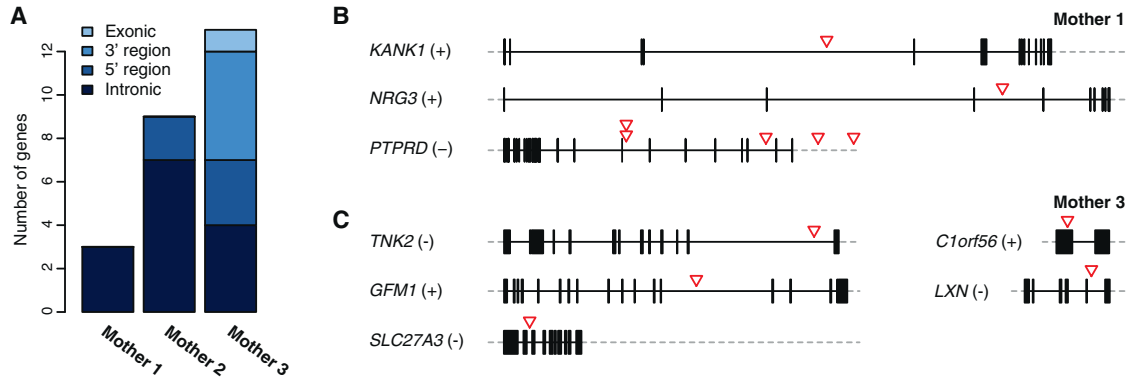

Figure 3. Chromothripsis Breakage Affects Protein-Coding Genes
(A) Number of genes affected by chromothripsis breakpoints in mothers 1, 2, and 3. Genes are considered affected if a break occurred in, or in close proximity (within <20 kb distance) to, the gene.
(B) Three genes are disrupted by breakpoints in mother 1; red arrowheads indicate the location of the break.
(C) Five out of 13 genes affected by breakpoints in mother 3.

the mothers and the severe congenital phenotypes in their children. We used mate-pair sequencing and did not identify any de novo breakpoint junctions in the children, despite the presence of multiple unique copy-number changes. For family 1, 5 out of the 13 rearrangements were detected in both the mother and her child. These represent all junctions on der(9), whereas none of the breakpoint junctions on the other three derivative chromosomes present in mother 1 were detected in her child (Figure 1B, Figure 4A); these results are consistent with the G-banded chromosome analysis. Out of the 23 breakpoint junctions detected in mother 2, her son harbored 16, representing the complete der(7) and der(12) chromosomes, whereas none of the junctions on der(6), der(9), or der(10) were detected in him (Figure S5A, Figure 2B). These findings indicate that the children inherited a subset of derivative chromosomes from their mothers and did not acquire any additional breakpoints upon germline transfer. In support of this, partial inheritance of the chromothripsis chromosomes explains all de novo copy-number changes in children 1 and 2 (Figure S1, Figure 4A, Figure S5A). Remarkably, the interstitial deletion on chr9 of child 1 is a result of five distinct, sequential chromosomal fragments that have been inserted in der(10), which was not transmitted to this child (Figure 4B). Similarly, the three copy gains in 9p21–24 in child 2 are a direct consequence of the presence of eight, rather than three, distinct segments of chromosome 9 inserted into der(12) (Figure 4B). Finally, we examined the transmission of breakpoint junctions in family 3. Seven out of eight junctions identified in the mother were also detected in the child (Table S2). The breakpoint junction missing in the child flanks the de novo deletion on 1q21.3 and matches the loss of this segment from der(3) in the child (Figure S5B).[11] Unfortunately, we did not identify a de novo breakpoint junction that explains the terminal 3q29 duplication in child 3.

Previously detected CCRs in healthy individuals harbor relatively few breaks.[4] In contrast, the three mothers presented here show a 1.1- to 2.6-fold increase in the number of rearrangements compared to those of their severely affected children, indicating that a larger number of breakpoints does not necessarily lead to more severe disease. Thus, the massive genome breakage and reassembly that occurred in the mothers is not the primary determinant of the phenotypic consequences in their children. Instead, the congenital abnormalities in the three children are caused by the CNVs that resulted from the partial or unstable transmission of the chromothripsis chromosomes. In support of this, trisomy 16qter, which is found in child 1, has previously been found to cause severe psychomotor retardation, facial dysmorphisms, and multiple other congenital defects, including heart, skeletal, kidney, gall bladder, and genital abnormalities.[19,20] Most, if not all, abnormalities observed in this child can probably be attributed to the 27 Mb trisomy of 16qter. The phenotypes of children 2 and 3 can also largely be explained by their CNVs, as described previously.[10,11] For child 2, this is further supported by the findings in two of his siblings, who only share the mother's much milder phenotype and who did not harbor the chr9 duplications and chr12 deletions found in child 2 (Figure S6A). Interestingly, PCR and Sanger sequencing revealed that both siblings have also only partially inherited the chromothripsis chromosomes from their mother, albeit a different subset of them (Figure S6B). Like child 2, the siblings inherited der(7) and der(12) but not der(6) or der(10) from their mother; however, unlike child 2, they additionally inherited der(9), leading to copy-number balanced chr9 and chr12.

In conclusion, our results give important insights into the permissiveness of the human genome to extreme CCRs by demonstrating that it can tolerate massive chromothripsis rearrangements, disrupting multiple protein-coding genes, without phenotypic consequences. This suggests that chromothripsis, although rare, might be more common in the general population than previously expected. To date, ~100 apparently balanced CCRs have

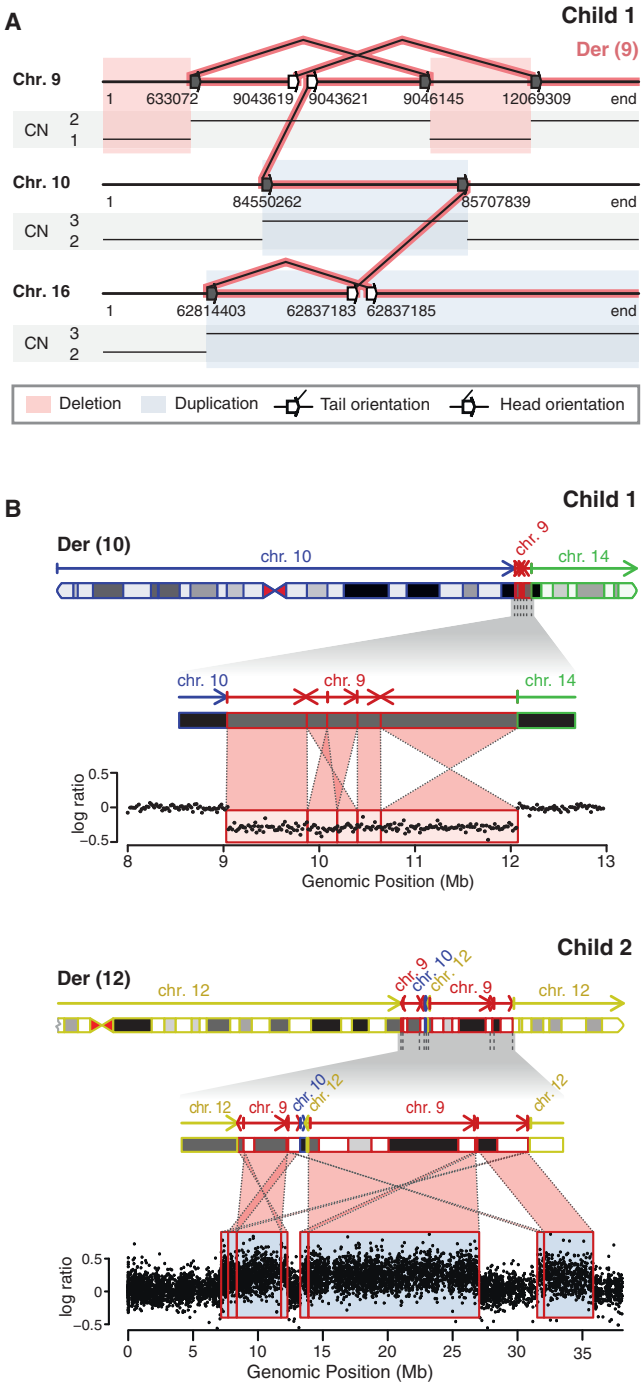

Figure 4. Stable but Partial Inheritance of Chromothripsis Chromosomes Can Lead to Highly Complex Copy-Number Changes

(A) Schematic representation of the breakpoint junctions detected in child 1. The CNVs detected in this child are explained by the structure of the inherited der(9). Connected lines between two arrows indicate breakpoint junctions. Adjacent white arrows indicate DSBs, and gray arrows indicate a single end of a break that was found to be a DSB in the mother. The other single end of these DSBs is located on der(10), der(14), or der(16), which were not inherited by the child, explaining the CNVs.

(B) Apparently simple CNVs can consist of multiple, highly rearranged, sequential chromosomal fragments rather than one solid fragment. Top: a deletion on chr9 in child 1 is a consequence of a highly complex rearrangement of five sequential chromosome fragments that were translocated to der(10) in the mother. Bottom: each of the three chr9 duplications detected in child 2 resulted from the translocation of multiple distinct chr9 segments into der(12) in the mother.

been described in phenotypically normal individuals experiencing a broad range of reproductive problems.[4] Some of these individuals might be affected by chromothripsis, given that the relatively low-resolution techniques used to identify these individuals are unable to uncover the full complexity of their CCRs.

In line with previous findings, including the fact that the presence of a CCR often leads to infertility in males, the chromothripsis chromosomes in this study are transferred from mother to child.[3] We demonstrate that chromothripsis in healthy females can severely impact reproduction by causing miscarriages, abortions, and the birth of children with multiple congenital abnormalities and developmental delay (Table S1). The copy-number-neutral character of the chromothripsis rearrangements found in the mothers in this study shows the necessity of the use of a combination of detection methods rather than the use of CNV analysis alone for couples experiencing a broad range of reproductive problems.

Accession Numbers

The accession number for the microarray data reported in this paper is GSE65454 (NCBI Gene Expression Omnibus). The accession number for the mate-pair sequencing data reported in this paper is PRJEB8343 (European Nucleotide Archive).

Supplemental Data

Supplemental Data include six figures and four tables and can be found online at http://dx.doi.org/10.1016/j.ajhg.2015.02.005.

Acknowledgments

We are grateful to the families for participating in this study. This research was supported by the Child Health priority program at the University Medical Center Utrecht. We thank M.E.M. Swinkels and E.F. Ippel for counseling family 2 and family 3, respectively. We would like to thank M. Poot for providing access to SNP array data for family 2.

Received: December 12, 2014
Accepted: February 5, 2015
Published: March 19, 2015

Web Resources

The URLs for data presented herein are as follows:

Ensembl Genome Browser, http://www.ensembl.org/index.html
European Nucleotide Archive (ENA), http://www.ebi.ac.uk/ena
ExAC Browser, http://exac.broadinstitute.org/
Gene Expression Omnibus (GEO), http://www.ncbi.nlm.nih.gov/geo
OMIM, http://www.omim.org/

References

1. Batista, D.A., Pai, G.S., and Stetten, G. (1994). Molecular analysis of a complex chromosomal rearrangement and a review of familial cases. Am. J. Med. Genet. *53*, 255–263.
2. Gorski, J.L., Kistenmacher, M.L., Punnett, H.H., Zackai, E.H., and Emanuel, B.S. (1988). Reproductive risks for carriers of complex chromosome rearrangements: analysis of 25 families. Am. J. Med. Genet. *29*, 247–261.
3. Pellestor, F., Anahory, T., Lefort, G., Puechberty, J., Liehr, T., Hédon, B., and Sarda, P. (2011). Complex chromosomal rearrangements: origin and meiotic behavior. Hum. Reprod. Update *17*, 476–494.
4. Madan, K. (2012). Balanced complex chromosome rearrangements: reproductive aspects. A review. Am. J. Med. Genet. A. *158A*, 947–963.
5. Stephens, P.J., Greenman, C.D., Fu, B., Yang, F., Bignell, G.R., Mudie, L.J., Pleasance, E.D., Lau, K.W., Beare, D., Stebbings, L.A., et al. (2011). Massive genomic rearrangement acquired in a single catastrophic event during cancer development. Cell *144*, 27–40.
6. Chiang, C., Jacobsen, J.C., Ernst, C., Hanscom, C., Heilbut, A., Blumenthal, I., Mills, R.E., Kirby, A., Lindgren, A.M., Rudiger, S.R., et al. (2012). Complex reorganization and predominant non-homologous repair following chromosomal breakage in karyotypically balanced germline rearrangements and transgenic integration. Nat. Genet. *44*, 390–397, S1.
7. Kloosterman, W.P., Guryev, V., van Roosmalen, M., Duran, K.J., de Bruijn, E., Bakker, S.C., Letteboer, T., van Nesselrooij, B., Hochstenbach, R., Poot, M., and Cuppen, E. (2011). Chromothripsis as a mechanism driving complex de novo structural rearrangements in the germline. Hum. Mol. Genet. *20*, 1916–1924.
8. Kloosterman, W.P., Tavakoli-Yaraki, M., van Roosmalen, M.J., van Binsbergen, E., Renkens, I., Duran, K., Ballarati, L., Vergult, S., Giardino, D., Hansson, K., et al. (2012). Constitutional chromothripsis rearrangements involve clustered double-stranded DNA breaks and nonhomologous repair mechanisms. Cell Rep. *1*, 648–655.
9. Zhang, C.Z., Leibowitz, M.L., and Pellman, D. (2013). Chromothripsis and beyond: rapid genome evolution from complex chromosomal rearrangements. Genes Dev. *27*, 2513–2530.
10. de Pater, J.M., Ippel, P.F., van Dam, W.M., Loneus, W.H., and Engelen, J.J. (2002). Characterization of partial trisomy 9p due to insertional translocation by chromosomal (micro) FISH. Clin. Genet. *62*, 482–487.
11. van Binsbergen, E., Hochstenbach, R., Giltay, J., and Swinkels, M. (2012). Unstable transmission of a familial complex chromosome rearrangement. Am. J. Med. Genet. A. *158A*, 2888–2893.
12. Francioli, L.C., Menelaou, A., Pulit, S.L., Van Dijk, F., Palamara, P.F., Elbers, C.C., Neerincx, P.B.T., Ye, K., Guryev, V., Kloosterman, W.P., et al.; Genome of the Netherlands Consortium (2014). Whole-genome sequence variation, population structure and demographic history of the Dutch population. Nat. Genet. *46*, 818–825.
13. Korbel, J.O., and Campbell, P.J. (2013). Criteria for inference of chromothripsis in cancer genomes. Cell *152*, 1226–1236.
14. Macera, M.J., Sobrino, A., Levy, B., Jobanputra, V., Aggarwal, V., Mills, A., Esteves, C., Hanscom, C., Pereira, S., Pillalamarri, V., et al. (2014). Prenatal diagnosis of chromothripsis, with nine breaks characterized by karyotyping, FISH, microarray and whole-genome sequencing. Prenat. Diagn. Published online July 9, 2014. http://dx.doi.org/10.1002/pd.4456.
15. Nazaryan, L., Stefanou, E.G., Hansen, C., Kosyakova, N., Bak, M., Sharkey, F.H., Mantziou, T., Papanastasiou, A.D., Velissariou, V., Liehr, T., et al. (2014). The strength of combined cytogenetic and mate-pair sequencing techniques illustrated by a germline chromothripsis rearrangement involving FOXP2. Eur. J. Hum. Genet. *22*, 338–343.
16. Kloosterman, W.P., and Cuppen, E. (2013). Chromothripsis in congenital disorders and cancer: similarities and differences. Curr. Opin. Cell Biol. *25*, 341–348.
17. Huang, N., Lee, I., Marcotte, E.M., and Hurles, M.E. (2010). Characterising and predicting haploinsufficiency in the human genome. PLoS Genet. *6*, e1001154.
18. MacArthur, D.G., Balasubramanian, S., Frankish, A., Huang, N., Morris, J., Walter, K., Jostins, L., Habegger, L., Pickrell, J.K., Montgomery, S.B., et al.; 1000 Genomes Project Consortium (2012). A systematic survey of loss-of-function variants in human protein-coding genes. Science *335*, 823–828.
19. Laus, A.C., Baratela, W.A., Laureano, L.A., Santos, S.A., Huber, J., Ramos, E.S., Rebelo, C.C., Squire, J.A., and Martelli, L. (2009). Karyotype/phenotype correlation in partial trisomies of the long arm of chromosome 16: case report and review of literature. Am. J. Med. Genet. A *158A*, 821–827.
20. Brisset, S., Joly, G., Ozilou, C., Lapierre, J.M., Gosset, P., Le-Lorc'h, M., Raoul, O., Turleau, C., Vekemans, M., and Romana, S.P. (2002). Molecular characterization of partial trisomy 16q24.1-qter: clinical report and review of the literature. Am. J. Med. Genet. *113*, 339–345.

The American Journal of Human Genetics

Supplemental Data

Chromothripsis in Healthy Individuals Affects Multiple Protein-Coding Genes and Can Result in Severe Congenital Abnormalities in Offspring

Mirjam S. de Pagter, Markus J. van Roosmalen, Annette F. Baas, Ivo Renkens, Karen J. Duran, Ellen van Binsbergen, Masoumeh Tavakoli-Yaraki, Ron Hochstenbach, Lars T. van der Veken, Edwin Cuppen, and Wigard P. Kloosterman

Supplemental Figures

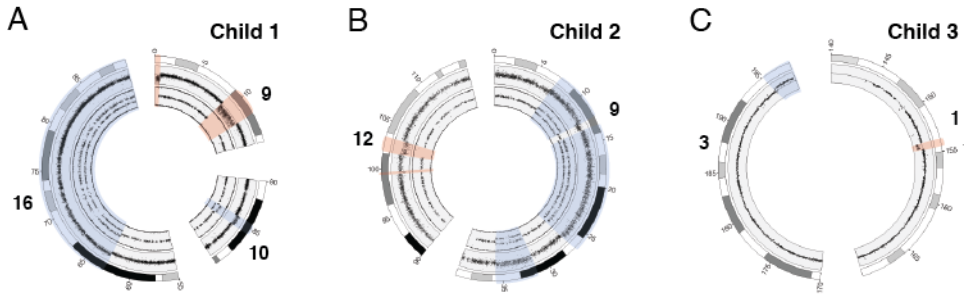

Figure S1. Circos plots displaying CNVs identified in child 1 (A), 2 (B) and 3 (C). CNVs were detected using Illumina SNParrays (CytoSNP-850K for case 1 and HumanCNV370 arrays for case 2) or custom Agilent 105k microarrays (Amadid 019015; case 3). Deletions and duplications were detected using Nexus software and are highlighted in red and blue, respectively. (A) Circos plot displaying two deletions (0.5 and 3 Mb) on chromosome 9, a 1.1 Mb duplication on chromosome 10 and a duplication of ~27 Mb on chromosome 16 in child 1. (B) In child 2, three duplications on chromosome 9 (4.5, 12 and 3 Mb) and two deletions on chromosome 12 (150 kb and 2 Mb) were detected by SNP array analysis. Previously published data, deposited in the NCBI Gene Expression Omnibus under accession number GSE37906[8]. (C) A 0.7 Mb deletion on chromosome 1 and a 2.3 Mb duplication on chromosome 3 were detected in child 3.

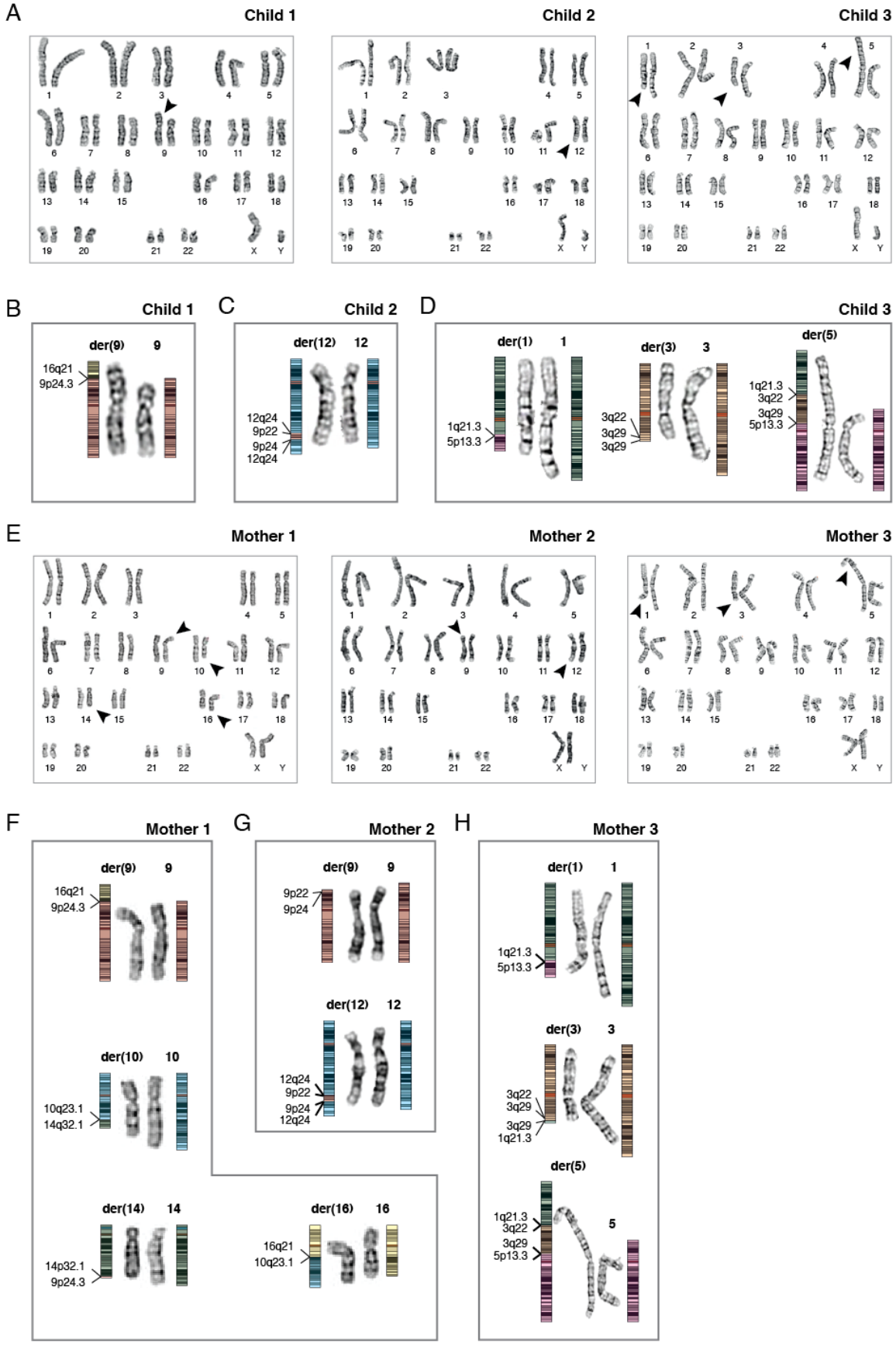
A
Child 1
Child 2
Child 3
B
Child 1
der(9) 9
16q21
9p24.3
C
Child 2
der(12) 12
12q24
9p22
9p24
12q24
D
Child 3
der(1) 1
1q21.3
5p13.3
der(3) 3
3q22
3q29
3q29
der(5)
1q21.3
3q22
3q29
5p13.3
E
Mother 1
Mother 2
Mother 3
F
Mother 1
der(9) 9
16q21
9p24.3
der(10) 10
10q23.1
14q32.1
der(14) 14
14p32.1
9p24.3
der(16) 16
16q21
10q23.1
G
Mother 2
der(9) 9
9p22
9p24
der(12) 12
12q24
9p22
9p24
12q24
H
Mother 3
der(1) 1
1q21.3
5p13.3
der(3) 3
3q22
3q29
3q29
1q21.3
der(5)
1q21.3
3q22
3q29
5p13.3
5

Figure S2. Karyograms of the children and mothers. (A) Karyogram of child 1, 2 and 3. (B-D) Partial karyograms and schematic diagrams of derivative chromosomes detected in child 1 (B), 2 (C) and 3 (D). (E) Karyogram of mother 1, 2 and 3. (F-H) Partial karyograms and schematic diagrams of the derivative chromosomes detected in mother 1 (F), 2 (G) and 3 (H).

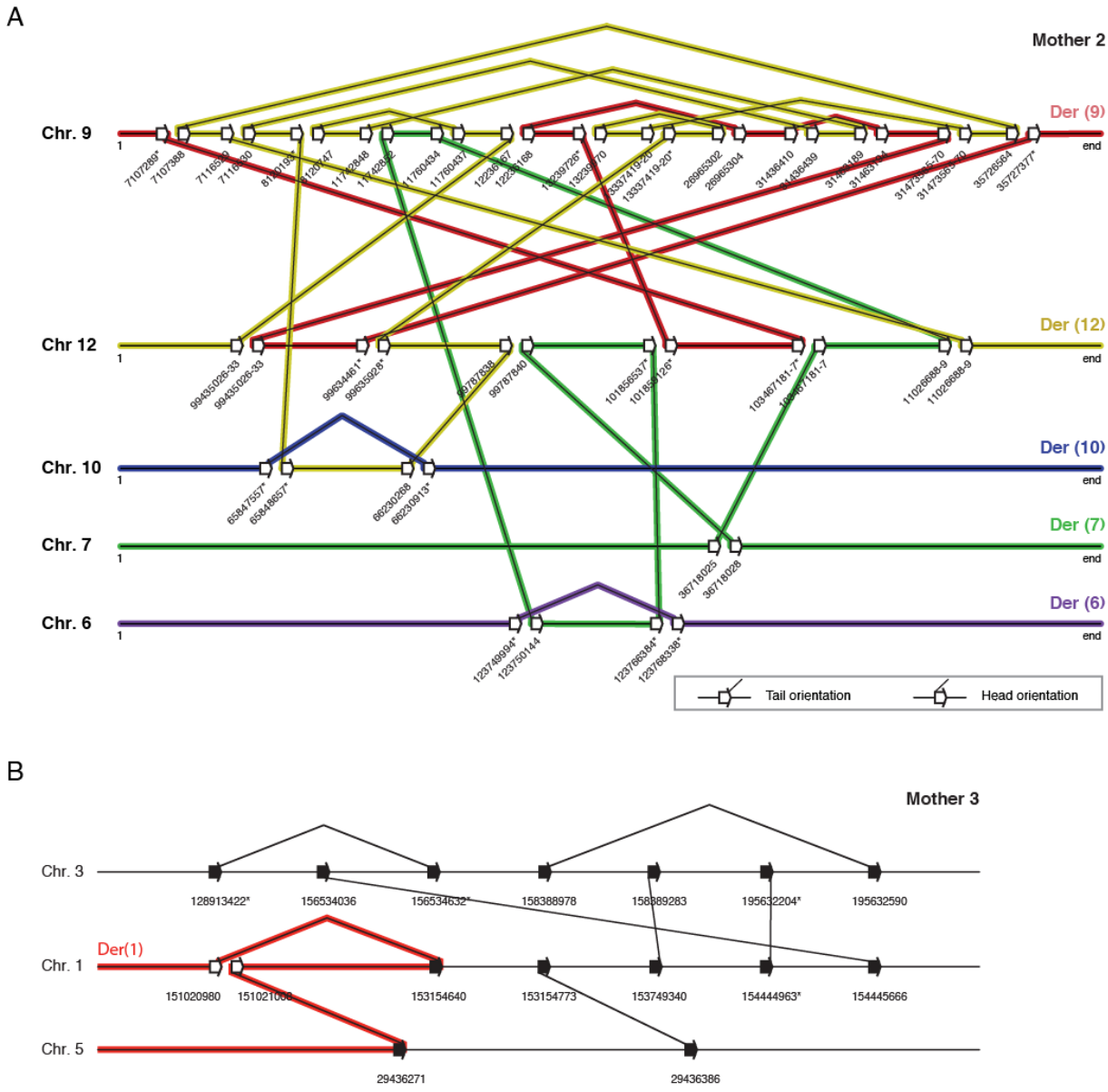

Figure S3. Schematic diagram showing the genomic positions and orientations of breakpoint junctions in mother 2 (A) and 3 (B). Sets of adjacent white arrows indicate a double-strand break (DSB), connecting lines between two arrows indicate breakpoint junctions. (A) Mate-pair sequencing revealed 23 breakpoint junctions involving five chromosomes in mother 2. Colored lines indicate predicted derivative chromosomes. The rearrangements gave rise to five derivative chromosomes der(6) (purple), der(7) (green), der(9) (red), der(10) (blue) and der(12) (yellow). Previously published data, deposited in the European Nucleotide Archive under accession number ERP001035 [8]. (B) Mate-pair sequencing revealed at least 8 breakpoint junctions involving three chromosomes in mother 3. Due to the repetitive nature of the 3q29 region involved in the rearrangements we were unable to fully reconstruct the derivative chromosomes for this individual.

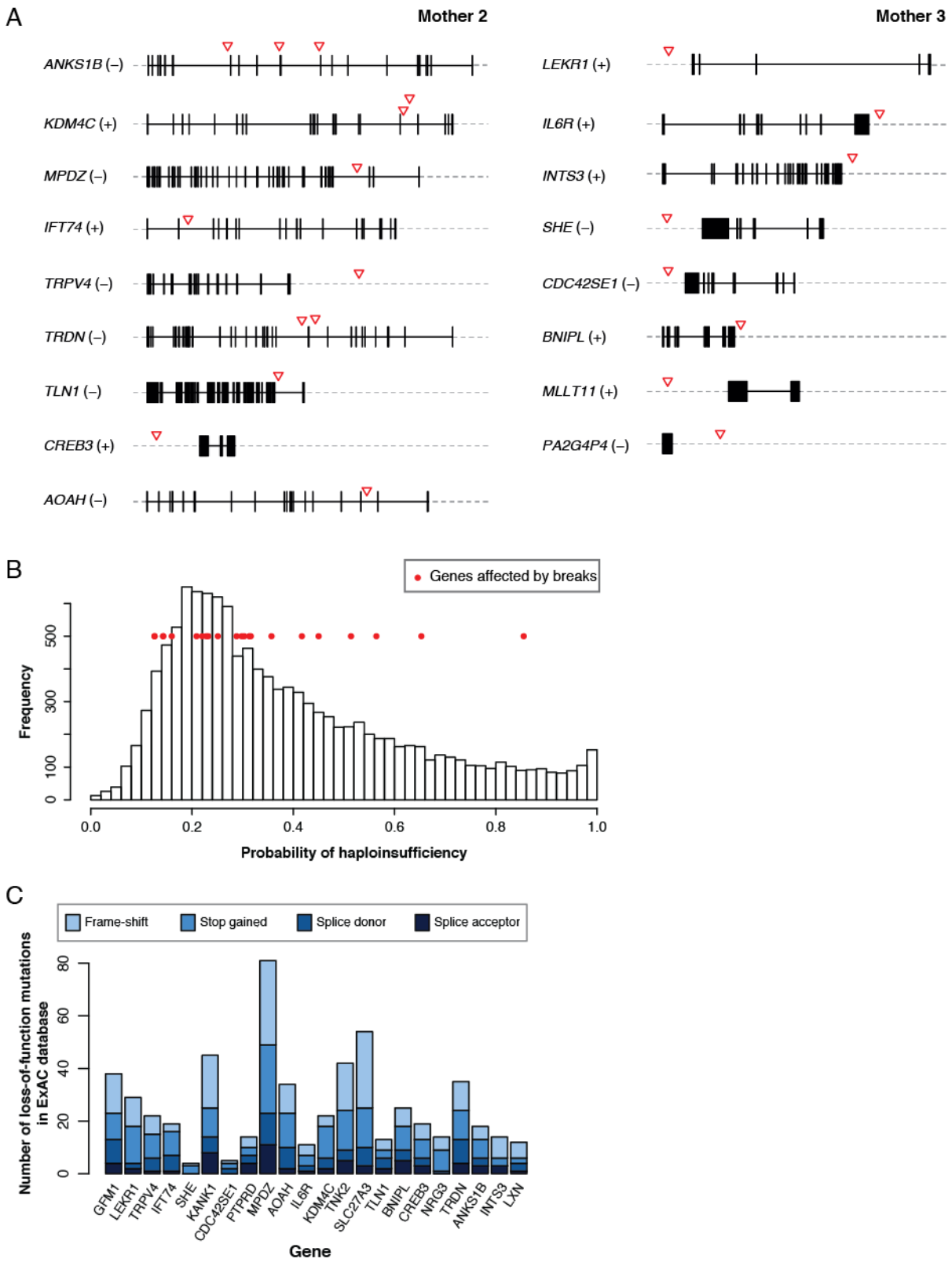

Figure S4. Chromothripsis directly affects protein-coding genes. (A) Gene structure and indication of breakpoint positions (triangles). (B) Predicted probability of haploinsufficiency for all genes affected by

chromothripsis breakpoints (red dots) relative to 12,218 genes in the genome (histogram)[17]. (C) Presence of loss-of-function mutations in genes affected by chromothripsis breakpoints. Loss-of-function mutations are derived from the exome aggregation consortium.

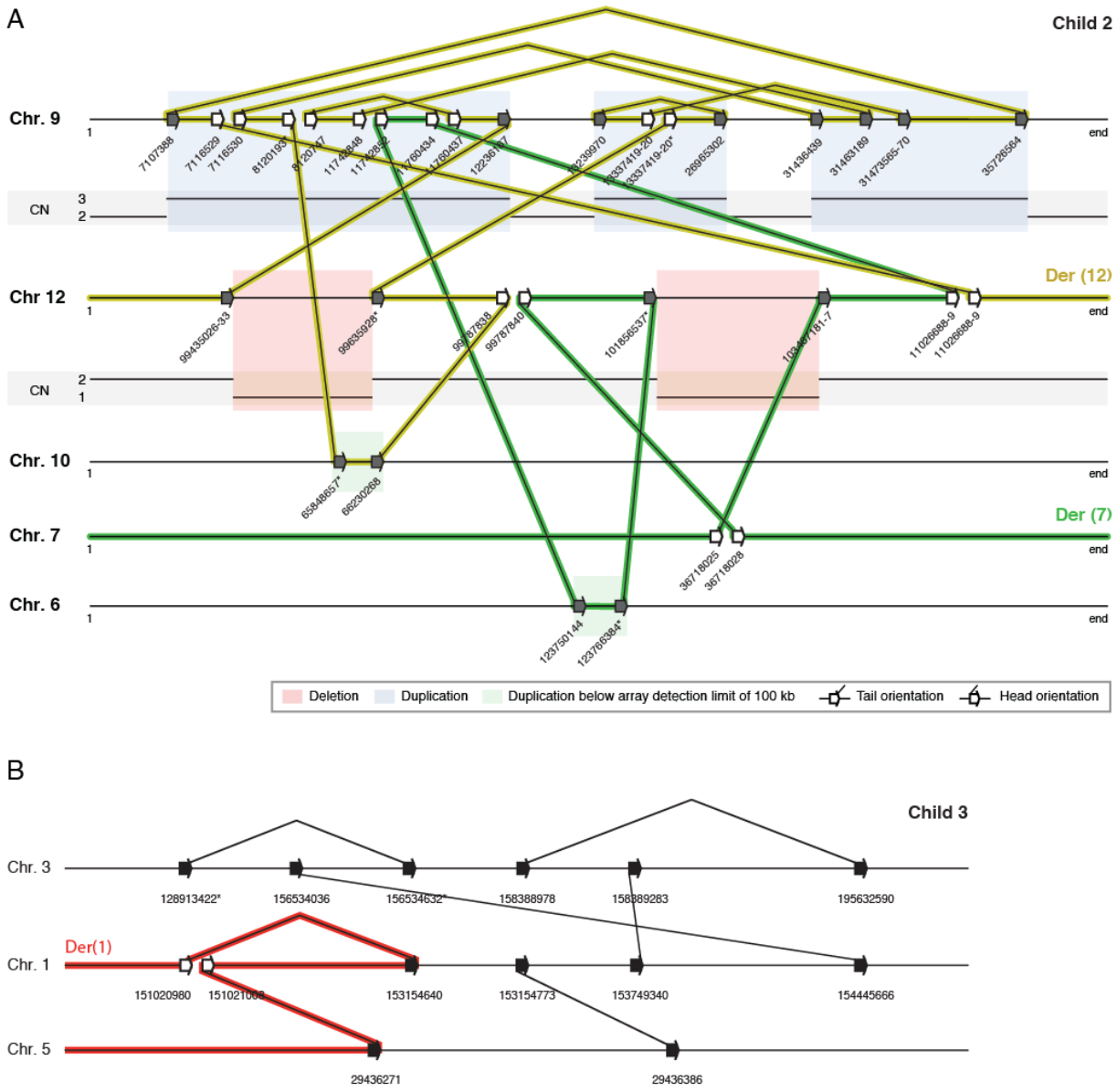

Figure S5. Rearrangements detected in child 2 and 3. Sets of adjacent white arrows indicate a double-strand break (DSB), grey arrows indicate a single end of a break that was found to be a DSB in the mother. Connecting lines between two arrows indicate breakpoint junctions. (A) Mate-pair sequencing revealed 16 breakpoint junctions in child 2. The chromosome 9 duplications can be explained by the presence of these fragments on der(12), which was inherited by the child. The deleted fragments of chromosome 12 are located on der(9), which was not inherited. Previously published data, deposited in the European Nucleotide Archive under accession number ERP001035 [8]. (B) 7 Breakpoint junctions were detected in child 3. The presence of the chromothripsis rearrangements in the mother gave rise to unstable transfer of the chromothripsis chromosomes to her child. All but one breakpoint junctions detected in the mother were also detected in her child. Due to the repetitive nature of the 3q29 region involved in the rearrangements we could not fully reconstruct the derivative chromosomes in this child.

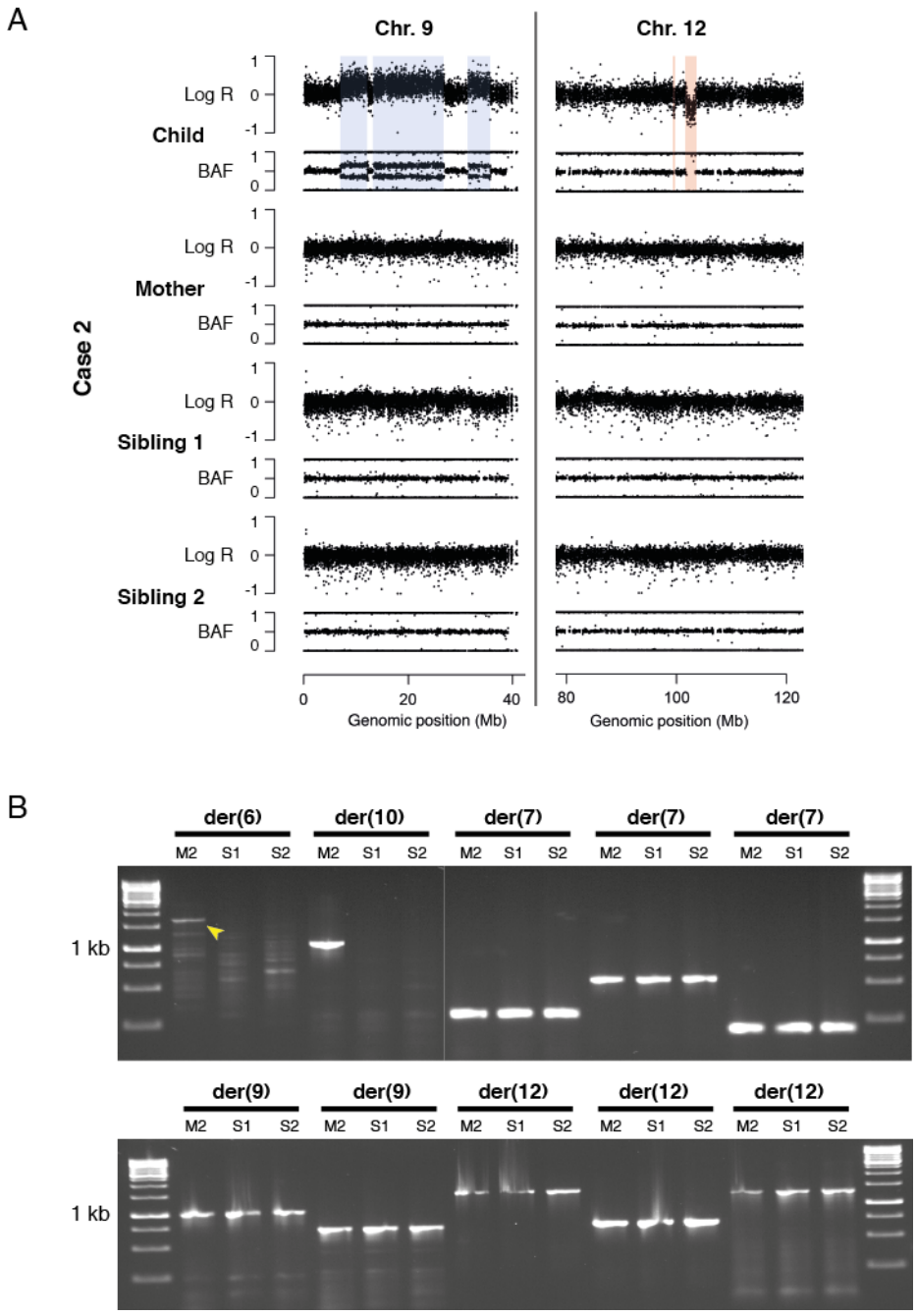

Figure S6. PCR and SNP array results for the two siblings of child 2. Partial inheritance of a different subset of chromothripsis chromosomes from the mother leads to a more copy number balanced state in two siblings of child 2. (A) SNP array results for the child, mother and two siblings in case 2. Child 2 carries three duplications on chromosome 9 and two deletions on chromosome 12 which are unique to this child. (B) PCR and Sanger sequencing revealed both siblings, like child 2, also inherited der(7) and der(12) and not der(6) and der(10) from their mother; however, unlike child 2, they additionally inherited der(9), leading to the copy neutral state of chromosome 9 and 12. Abbreviations are as follows: M2, mother 2; S1, sibling 1; S2, sibling 2.

Supplemental Tables

Table S1. Phenotypic and genomic characteristics of the children and mothers described in this study. Coordinates are in hg19. Abbreviations are as follows: C, child; M, mother; MP-seq, mate-pair sequencing.

C/M	Clinical phenotype	Birth/pregnancy history	Cytogenetic result	# of breakpoint junctions detected (MP-seq)	Chromosomes involved
C1	Ambiguous genitals; prominent forehead; hyperteloric; downslant; periorbital oedemia; beaked nose; thin lips; low-set ears; pointy chin; clinidactyly 5th digits; right foot: syndactyly (2nd-3rd digits), 2 rudimentary digits (4th and 5th). Li- g.b; asymmetrically enlarged ventricles, gallbladder agenesis; multiple VSDs and open ductus, hypotonic	1st pregnancy, caesarean section at 34.7 weeks of gestation Birth weight: 1900g (10th centile) Birth length: unknown Head circumference: 31 cm (10th centile)	46,XY,der(9)t(9;14;10;16)(p24.3;q32.1;q23.1;q21)mat.arr 9p24.3(193,993-615,714)x1,9p23(9,043,125-12,048,982)x1,10q23.1(84,551,375-85,687,314)x3,16q21q24.3(61,374,670-88,690,771)x3	5	9, 10, 14, 16
M1	No clinical phenotype	1.5 years until first pregnancy, no miscarriages/spontaneous abortions, PCOS; 6 ovolutations a year	46,XX,t(9;14;10;16)(p24.3;q32.1;q23.1;q21)	13	9, 10, 14, 16
C2	Severe mental and growth retardation, microcephaly, epicanthus, low-set ears, micrognatia, clinodactyly and hypoplastic phalanges of the fifth fingers, hypoplasia or absence of toenails, and extremely small genitals (For detailed description see: de Pater et al[10])	2nd pregnancy, uneventful and ended at 38.2 weeks of gestation. Birth weight: 2570g(<3rd centile) Birth length: 49 cm (25 centile) Head circumference: 32 cm (<3rd centile) [10]	46,XY,der(12)-ins(12;9)(q24.1;p22p24)mat.arr 9p23-p24.1(7,143,431-12,234,642)x3,9p21.2-p23(13,300,367-26,978,170)x3,9p31.3-p21.1(31,591,132-35,648,008)x3, 12q23.1(99,435,026-99,635,928)x1, 12q23.2(101,916,750-103,544,418)x1[10]	16	6, 7, 9, 10, 12
M2	Delayed psychomotor development and major learning difficulties, no dysmorphic features[10]	No history of previous miscarriages/ spontaneous abortions, 1st and 3rd pregnancy ended in the birth of male infants sharing only the mothers' phenotype[10]	46,XX,ins(12;9)(q24.1;p22p24) [10]	23	6, 7, 9, 10, 12
C3	Hypotonia, mild facial dysmorphisms, severe psychomotor development, non-progressie white matter abnormalities, small hands with single transverse creases, feeding difficulties, recurrent upper airway infections, and severe intellectual disability (For detailed description see: van Binsbergen et al[11])	3rd pregnancy, ended at 38 weeks of gestation Birth weight: 2,425 g (5th centile) Birth length: 50 cm (50th centile) Head circumference: 36 cm (80th centile) [11]	46,XY, der(1)(1pter->1q21.3::5p13.3->5pter),der(3)(3pter -> 3q22::3q29-> 3qter::3q29-> 3qter),der(5)(1qter -> 1q21.3::3q22 -> 3q29::5p13.3 -> 5qter).arr1q21.3(153751264-154439066) x 1,3q29(195420586-197837049) x 3 dn[11]	7	1, 3, 5
M3	No clinical phenotype[11]	One previous elective abortion and one early miscarriage[11]	46,XX, der(1)(1pter->1q21.3::5p13.3->5pter),der(3)(3pter -> 3q22::3q29 -> 3qter::1q21.3 -> 1q21.3:),der(5)(1qter -> 1q21.3::3q22 -> 3q29::5p13.3 -> 5qter). arr(1-22,X) x 2[11]	8	1, 3, 5

Table S2. Breakpoint junctions detected in all three cases (mothers and children) by mate-pair sequencing and PCR and Sanger sequencing. Additional information per column:

[a] For every breakpoint junction our analysis pipeline specifies the coordinates of the boundaries of the two genomic fragments that are connected together. Coordinates represent the outer boundaries derived from all mate-pair clones supporting the breakpoint junction. Chr1, s1 and e1 specify the chromosome and left and right coordinate of the first fragment respectively. Similarly chr2, s2 and e2 specify the chromosome and coordinates of the second fragment.

[b] Individuals the specific breakpoint junction was detected in: M, mother; F, father; C, child. Count represents the number of reads covering the breakpoint junction.

[c] Orientation of the breakpoint (BP) junction between the two chromosomal fragments specified in each row. A fragment can be detected at its head (H) or tail (T) side to another fragment. The first letter (H or T) indicates the orientation of fusion of the first fragment (chr1, s1, e1) and the second letter indicates the fusion orientation of the second fragment (chr2, s2, e2).

[d] Total number of unique mate-pair reads supporting the breakpoint junction. All reads were uniquely identified in the indicated mother and or child and not in any of 150 control mate-pair datasets.

[e] For every breakpoint junction, chr1 and bp1 indicate the exact breakpoint location of the first, and chr2 and bp2 that of the second of the two fragments that are connected together at the specific breakpoint junction. Abbreviations are as follows: nd, not detected by PCR; nt, not tested by PCR.

[f] Individuals the breakpoint junction was confirmed in by PCR and Sanger sequencing; M, mother; C, child.

[g] Characteristics of the breakpoint junction. Chromosomal fragments can be either fused blunt, the connection can be guided by microhomologous sequences at either end of the junction or a few (non-templated) nucleotides can be inserted between the two connected ends. Bp change represents microhomology or inserted sequence found at the breakpoint junction.

[h] PCR products for these breakpoint junctions were >1.5 kb, which exceeds the maximum read length of Sanger sequencing (~650 bp). Sequencing using the forward primer identified the first fragment, the reverse primer identified the second fragment of the breakpoint junction.

	Mate-Pair sequencing results									PCR and Sanger sequencing results						
Case	chr1[a]	s1[a]	e1[a]	chr2[a]	s2[a]	e2[a]	Individual (counts)[b]	BP junction orientation[c]	Total count[d]	chr1[e]	bp1[e]	chr2[e]	bp2[e]	Bp conf.[f]	Breakpoint signature[g]	Bp change[g]
case 1	9	10640282	10641388	9	12067163	12069048	M(4)F(0)C(0)	TT	4	9	10642756	9	12069307	M	Microhomology	A
case 1	10	85708440	85709723	16	62811907	62813013	M(4)F(0)C(0)	HT	4	10	85707849	16	62814401	M	Blunt	-
case 1	9	10643066	10645130	14	87959160	87960589	M(7)F(0)C(0)	HH	7	9	10642768	14	87958400	M	Insertion	T
case 1	9	9874447	9875887	9	10397725	10400216	M(8)F(0)C(0)	TT	8	9	9876859	9	10400356	M	Microhomology	TGTCAT
case 1	9	9877636	9880121	9	10184962	10187413	M(11)F(0)C(0)	HH	11	9	9876864	9	10184654	M	Microhomology	GA
case 1	16	62814654	62819507	16	62837225	62840110	M(2)F(0)C(15)	HH	17	16	62814403	16	62837185	C,M	Microhomology	T
case 1	9	9039041	9043602	9	12069501	12073773	M(5)F(0)C(16)	TH	21	9	9043619	9	12069309	C,M	Blunt	-
case 1	9	633474	636448	9	9043966	9046015	M(2)F(0)C(19)	HT	21	9	633072	9	9046145	C,M	Blunt	-
case 1	9	9043986	9045832	10	84550840	84554624	M(2)F(0)C(24)	HH	26	9	9043621	10	84550262	C,M	Microhomology	A
case 1	10	85704055	85707766	16	62832514	62837165	M(8)F(0)C(29)	TT	37	10	85707839	16	62837183	C,M	Insertion	T
case 1	14	87956251	87957402	9	630972	632755	M(3)F(0)C(0)	TT	3	14	87958400	9	633072	M	Blunt	-
case1	10	84549834	84549834	9	9048033	9048033	M(1)F(0)C(0)	TH	1	10	84550260	9	9046159	M	Blunt	-
case1	9	10182312	10184604	9	10400974	10404035	M(7)F(0)C(0)	TH	7	9	10184643	9	10400358	M	Blunt	-

case 2	7	36718108	36721671	12	99787831	99790893	M(11)F(0)C(10)	HH	21	7	36718028	12	99787840	C,M	Microhomology	G
case 2	9	11739802	11742710	9	31460247	31463007	M(4)F(0)C(3)	TT	7	9	31463189	9	11742848	C,M	Blunt	-
case 2	9	11758195	11759972	12	110263742	110266538	M(3)F(0)C(2)	TT	5	9	11760434	12	110266889	C,M	Blunt	-
case 2	9	7104763	7106960	12	103464346	103466774	M(11)F(0)C(0)	TT	11	9	7107289	12	103467187	M	Flanks identified[h]	-
case 2	9	12236188	12238989	9	26965673	26968013	M(10)F(0)C(0)	HH	10	9	12236168	9	26965304	M	Microhomology	TTG
case 2	9	13236665	13239425	12	101859464	101861141	M(7)F(0)C(0)	TH	7	9	13239726	12	101859126	M	Flanks identified[h]	-
case 2	6	123750357	123752276	9	11743072	11746336	M(9)F(0)C(3)	HH	12	6	123750144	9	11742852	C,M	Microhomology	A
case 2	6	123765872	123766384	12	101856510	101856537	M(2)F(0)C(0)	TT	2	nd	nd	nd	nd	nd	-	-
case 2	9	31433337	31436333	9	31463517	31465231	M(4)F(0)C(0)	TH	4	9	31436410	9	31463194	M	Microhomology	GA
case 2	9	31471300	31473229	12	99435218	99436825	M(6)F(0)C(0)	TH	6	9	31473570	12	99435026	M	Blunt	-
case 2	6	123748945	123750012	6	123768304	123769906	M(6)F(0)C(0)	TH	6	6	123749994	6	123768338	M	Flanks identified[h]	-
case 2	10	66227201	66230197	12	99785257	99787355	M(3)F(0)C(2)	TT	5	10	66230268	12	99787838	C,M	Complex	-
case 2	9	8118030	8119888	10	65848657	65850658	M(2)F(0)C(2)	TH	4	9	8120193	10	65848657	C,M	Only one flank identified	-
case 2	7	36714976	36717979	12	103467238	103470137	M(5)F(0)C(7)	TH	12	7	36718025	12	103467181	C,M	Blunt	-
case 2	9	7107641	7109780	9	35723601	35726283	M(8)F(0)C(6)	HT	14	9	7107388	9	35726564	C,M	Microhomology	A
case 2	9	13334672	13337076	9	31473792	31476201	M(6)F(0)C(5)	TH	11	9	13337420	9	31473565	C,M	Microhomology	TT
case 2	9	13240004	13241557	9	26962041	26964677	M(2)F(0)C(4)	HT	6	9	13239970	9	26965302	C,M	Blunt	-
case 2	9	7116561	7120299	9	31436447	31440029	M(7)F(0)C(5)	HH	12	9	7116530	9	31436439	C,M	Blunt	-
case 2	9	8121313	8122780	9	11760865	11763707	M(5)F(0)C(4)	HH	9	9	8120747	9	11760437	C,M	Microhomology	TGAG
case 2	9	12233990	12236078	12	99431406	99434124	M(11)F(0)C(6)	TT	17	9	12236167	12	99435033	C,M	Microhomology	G
case 2	9	7113602	7116395	12	110267135	110269429	M(10)F(0)C(6)	TH	16	9	7116529	12	110266889	C,M	Blunt	-
case 2	9	13337440	13340068	12	99636114	99638904	M(4)F(0)C6)	HH	10	9	13337419	12	99635928	C,M	Only one flank identified	-
case 2	10	65844061	65847557	10	66230913	66234003	M(7)F(0)C(0)	TH	7	nt	nt	nt	nt	nt	-	-
case 2	12	99634461	99634461	9	35727377	35727377	M(1)F(0)C(0)	TH	1	nt	nt	nt	nt	nt	-	-
case 3	3	158384939	158388876	3	195632595	195635632	M(8)F(0)C(6)	TH	14	3	158388978	3	195632590	C,M	Microhomology	GT
case 3	1	154441965	154444308	3	195630328	195631725	M(6)F(0)C(0)	TT	6	1	154444963	3	195632204	M	Flanks identified[h]	-
case 3	1	154445895	154448216	3	156530510	156533437	M(3)F(0)C(6)	HT	9	1	154445666	3	156534036	C,M	Microhomology	CG
case 3	1	153155549	153158347	5	29436496	29438223	M(10)F(0)C(3)	HH	13	1	153154773	5	29436386	C,M	Microhomology	AT
case 3	1	151021102	151023743	5	29433067	29436167	M(5)F(0)C(4)	HT	9	1	151021008	5	29436271	C,M	Microhomology	GC
case 3	3	128911732	128913422	3	156534632	156536932	M(8)F(1)C(2)	TH	11	nt	nt	nt	nt	nt	-	-
case 3	1	153746565	153748730	3	158389428	158392531	M(7)F(0)C(1)	TH	8	1	153749340	3	158389283	C,M	Microhomology	ACT
case 3	1	151018679	151020295	1	153151785	153154013	M(6)F(0)C(4)	TT	10	1	151020980	1	153154640	C,M	Insertion	TGGGAAGCTGCAC

Table S3. Comparison of the rearrangement characteristics for each of the three mothers to the criteria for inference of chromothripsis as defined by Korbel and Campbell[14]

Criteria for inference of chromothripsis	Mother 1	Mother 2	Mother 3
1. Clustering of breakpoints	+	+	+
2. Regularity of oscillating copy-number states	-	-	-
3. Prevalence of regions with interspersed loss and retention of heterozygosity	-	-	-
4. Prevalence of rearrangements affecting a single haplotype	+	+	+
5. Randomness of DNA segment order and fragment joins	+	+	+
6. Ability to 'walk' the derivative chromosome if all rearrangements in a region with chromothripsis are detectable	+	+	+[a]

[a] Due to the repetitive nature of one of the regions involved in the rearrangements we were unable to detect all breakpoints in this individual and could therefore not reconstruct all derivative chromosomes

Table S4. Effects of chromothripsis breakpoints on protein-coding genes.

Mother (case)	Gene symbol	Gene name	Breakpoint location[a]	Phenotype MIM number	Probability of haploinsufficiency[b]
1	*PTPRD*	PROTEIN-TYROSINE PHOSPHATASE, RECEPTOR-TYPE, DELTA	2 Breaks in intron; 2 breaks in 5' region of gene		0.855
1	*KANK1*	KN MOTIF- AND ANKYRIN REPEAT DOMAIN-CONTAINING PROTEIN 1	Break in intron	612900	0.653
1	*NRG3*	NEUREGULIN 3	Break in intron		0.251
2	*AOAH*	ACYLOXYACYL HYDROLASE	Break in intron		0.160
2	*ANKS1B*	ANKYRIN REPEAT AND STERILE ALPHA MOTIF DOMAINS-CONTAINING PROTEIN	3 Breaks in different introns		0.313
2	*TRPV4*	TRANSIENT RECEPTOR POTENTIAL CATION CHANNEL, SUBFAMILY V, MEMBER 4	Break in 5' region of gene	184095;181405;168400;156530;113500;184252;600175;613508;606835;606071	0.228
2	*KDM4C*	LYSINE-SPECIFIC DEMETHYLASE 4C	2 Breaks in intron		Not defined
2	*MPDZ*	MULTIPLE PDZ DOMAIN PROTEIN	Break in intron	615219	0.450
2	*IFT74*	INTRAFLAGELLAR TRANSPORT 74, CHLAMYDOMONAS, HOMOLOG OF	Break in intron		0.357
2	*TRDN*	TRIADIN	2 Breaks in intron	615441	0.288
2	*TLN1*	TALIN 1	Break in intron		0.417
2	*CREB3*	cAMP RESPONSE ELEMENT-BINDING PROTEIN 3	Break in 5' region of gene		0.298
3	*GFM1*		Break in intron		0.188
3	*LXN*	LATEXIN	Break in intron		0.303
3	*TNK2*	TYROSINE KINASE, NONRECEPTOR, 2	Break in intron		0.514
3	*SHE*	SH2 DOMAIN-CONTAINING PROTEIN E	2 Breaks in 3' regions of gene		0.143
3	*IL6R*	INTERLEUKIN 6 RECEPTOR	Break in 3' region of gene	614689;614752	0.209
3	*C1orf56*		Break in exon		0.143
3	*BNIPL*	BCL2/ADENOVIRUS E1B 19-KD PROTEIN-INTERACTING PROTEIN 2-LIKE	Break in 3' region of gene		Not defined
3	*CDC42SE1*		Break in 3' region of gene		0.316
3	*MLLT11*	MYELOID/LYMPHOID OR MIXED-LINEAGE LEUKEMIA, TRANSLOCATED TO, 11	Break in 5' region of gene		0.220
3	*LEKR1*	LEUCINE-, GLUTAMATE-, AND LYSINE-RICH PROTEIN 1	Break in 5' region of gene		0.232
3	*PA2G4P4*		Break in 5' region of gene		Not defined
3	*SLC27A3*	SOLUTE CARRIER FAMILY 27 (FATTY ACID TRANSPORTER), MEMBER 3	Break in intron		0.126
3	*INTS3*	INTEGRATOR COMPLEX SUBUNIT 3	Break in 3' region of gene		0.564

[a] We arbitrarily defined a 20kb region on the 5' and 3' part of the gene as the 5' and 3' region of the gene, respectively.

[b] Based on the method described by Huang et al.[17]